

Large Air Gap, Vibration-Tolerant, GMR Transmission Speed and Direction Sensor IC

FEATURES AND BENEFITS

- **GMR technology** delivers high magnetic sensitivity for large air gaps and minimal jitter
- **SolidSpeed Digital Architecture** provides robust, adaptive performance with advanced algorithms that provide vibration immunity over the full target pitch
- **Flexible orientation** allows parallel or perpendicular placement to the magnet
- **ISO 26262 ASIL B** with integrated diagnostics and certified safety design process
- **EEPROM** enables traceability throughout product life cycle



PACKAGE:



2-Pin SIP
(suffix UB)

Not to scale

DESCRIPTION

The A19571 is a magnetic sensor integrated circuit (IC) that uses giant magnetoresistance (GMR) technology to encode the speed and direction of rotating ring magnets. Using a state-of-the-art GMR stack design integrated with a BiCMOS process, the IC differentially measures magnetic fields and applies advanced digital processing to robustly measure ring magnets commonly used in automotive transmissions.

The A19571 features Allegro's SolidSpeed Digital Architecture for robust and reliable target tracking that adapts to changes in the air gap and the environment. Its advanced algorithms distinguish vibration from rotation to provide reliable speed and direction information to a controller.

The IC has been designed to a certified ISO 26262 design process to allow easy integration into high safety level systems. Integrated diagnostics are used to detect an IC failure that impacts the output protocol's accuracy, providing coverage compatible with ASIL B compliance.

The A19571 is provided in a 2-pin miniature SIP package (suffix UB) that is lead (Pb) free, with tin leadframe plating. The UB package includes an IC and capacitor integrated into a single overmolded package, with an additional molded lead-stabilizing bar for robust shipping and ease of assembly.

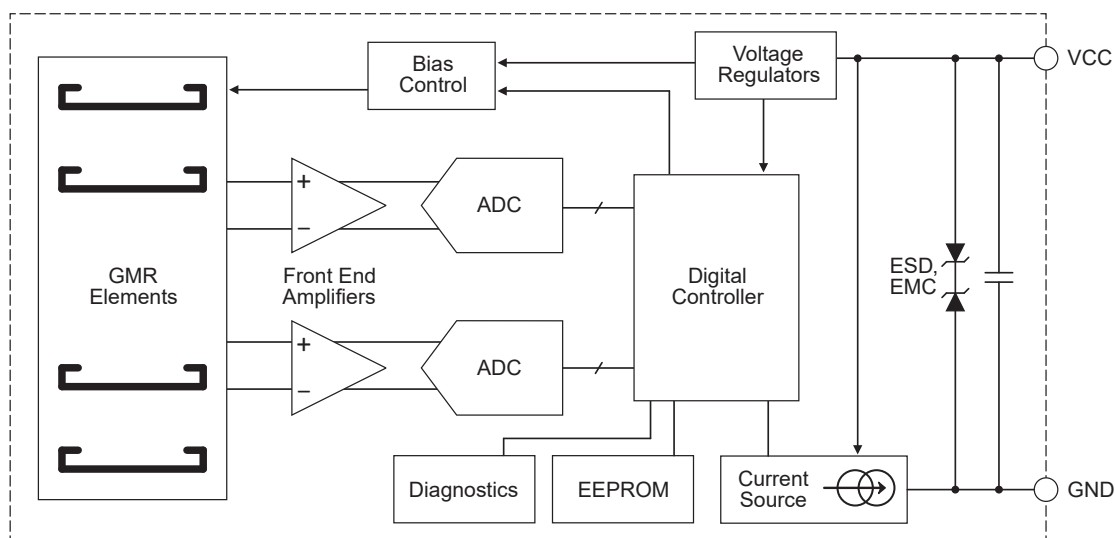


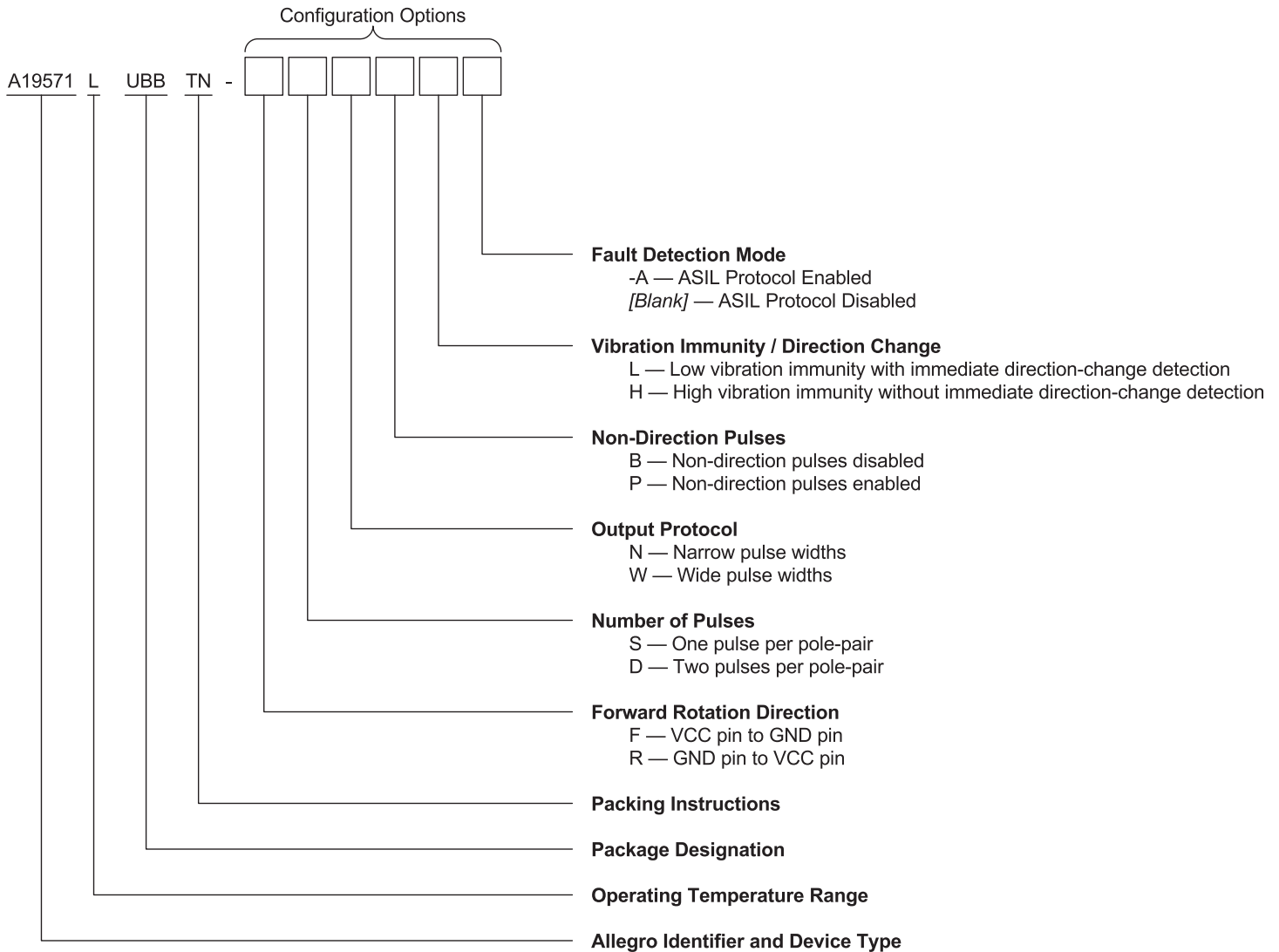
Figure 1: Functional Block Diagram

SELECTION GUIDE

SELECTION GUIDE*

Part Number	Packing
A19571LUBBTN-FSNPH	Tape and Reel, 4000 pieces per reel
A19571LUBBTN-RSNPH	

* Not all combinations are available. Contact Allegro sales for availability and pricing of custom programming options.



SPECIFICATIONS

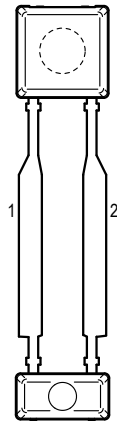
ABSOLUTE MAXIMUM RATINGS

Characteristic	Symbol	Notes	Rating	Unit
Supply Voltage	V_{CC}	Refer to Power Derating section	28	V
Reverse Supply Voltage	V_{RCC}		-18	V
Operating Ambient Temperature	T_A		-40 to 150	°C
Maximum Junction Temperature	$T_{J(max)}$		165	°C
Storage Temperature	T_{stg}		-65 to 170	°C
Applied Magnetic Flux Density	B	In any direction	500	G

INTERNAL DISCRETE CAPACITOR RATINGS

Characteristic	Symbol	Test Conditions	Value	Unit
Nominal Capacitance	C_{SUPPLY}	Connected between pin 1 and pin 2; see Figure 2	10	nF

PINOUT DIAGRAM AND TERMINAL LIST



Package UB, 2-Pin SIP Pinout Diagram

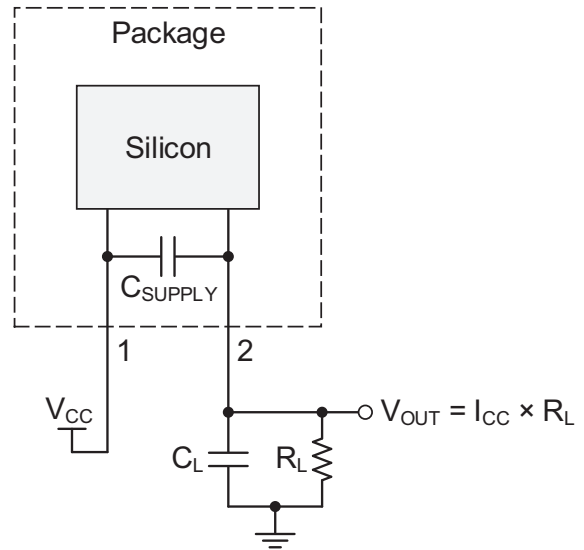


Figure 2: Application Circuit

Terminal List Table

Pin Name	Pin Number	Function
VCC	1	Supply Voltage
GND	2	Ground

OPERATING CHARACTERISTICS: Valid over operating voltage and temperature ranges, unless otherwise specified

Characteristic	Symbol	Test Conditions	Min.	Typ. [1]	Max.	Unit
ELECTRICAL CHARACTERISTICS						
Supply Voltage [2]	V_{CC}	Voltage across pin 1 and pin 2; does not include voltage across R_L	4	–	24	V
Undervoltage Lockout	$V_{CC(UV)}$		–	–	3.95	V
Reverse Supply Current [3]	I_{RCC}	$V_{CC} = -18$ V	-10	–	–	mA
Supply Zener Clamp Voltage	$V_{Zsupply}$	$I_{CC} = 19$ mA	28	–	–	V
Supply Current	$I_{CC(Low)}$	Low-current state	5.9	7	8.4	mA
	$I_{CC(High)}$	High-current state	12	14	16	mA
Supply Current Ratio [4]	$I_{CC(High)} / I_{CC(Low)}$	Ratio of high current to low current (isothermal)	1.9	–	–	–
ASIL Safety Current	I_{FAULT}		1.5	3	3.9	mA
POWER-ON CHARACTERISTICS						
Power-On State	POS	$V_{CC} > V_{CC(min)}$	$I_{CC(Low)}$			mA
Power-On Time [5]	t_{PO}	Time from $V_{CC} > V_{CC(min)}$, to when IC enters Calibration mode	–	–	1	ms
OUTPUT CHARACTERISTICS						
Output Rise, Fall Time	t_r, t_f	Voltage measured at device GND, see Typical Application Circuit; $R_L = 100 \Omega$, $C_L = 10$ pF, measured between 10% and 90% of the signal	–	2	4	μ s
Warning Fault Pulse Width [6]	$t_{w(FAULT,W)}$	Refer to Figure 13	–	90	–	μ s
Critical Fault Pulse Width [6]	$t_{w(FAULT,C)}$	Refer to Figure 13	3	–	6	ms

[1] Typical values are at $T_A = 25^\circ\text{C}$ and $V_{CC} = 12$ V. Performance may vary for individual units, within the specified maximum and minimum limits.

[2] Maximum voltage must be adjusted for power dissipation and junction temperature; see representative Power Derating section.

[3] Negative current is defined as conventional current coming out of (sourced from) the specified device terminal.

[4] Supply current ratio is taken as a mean value of $I_{CC(High)} / I_{CC(Low)}$.

[5] Output transients prior to t_{PO} should be ignored.

[6] Pulse width measured at threshold of $(I_{CC(High)} + I_{CC(Low)}) / 2$. ASIL Safe State Current Time is measured at the threshold of $(I_{FAULT} + I_{CC(Low)}) / 2$.

Continued on the next page...

**OPERATING CHARACTERISTICS (continued): Valid over operating voltage and temperature ranges,
unless otherwise specified**

Characteristic	Symbol	Test Conditions	Min.	Typ. [1]	Max.	Unit
NARROW PULSE WIDTH OPTION (-xSNxx VARIANTS)						
Forward Pulse Width [6]	$t_{w(FWD)}$		38	45	52	μs
Reverse Pulse Width [6]	$t_{w(REV)}$		76	90	104	μs
Nondirection Pulse Width [6]	$t_{w(ND)}$		153	180	207	μs
Operating Frequency, Forward Rotation [7]	f_{FWD}		0	–	12	kHz
Operating Frequency, Reverse Rotation [7]	f_{REV}		0	–	7	kHz
Operating Frequency, Nondirection Pulses [7]	f_{ND}		0	–	4	kHz
WIDE PULSE WIDTH OPTION (-xSWxx VARIANTS)						
Forward Pulse Width [6]	$t_{w(FWD)}$		38	45	52	μs
Reverse Pulse Width [6]	$t_{w(REV)}$		153	180	207	μs
Nondirection Pulse Width [6]	$t_{w(ND)}$		306	360	414	μs
Operating Frequency, Forward Rotation [7]	f_{FWD}		0	–	12	kHz
Operating Frequency, Reverse Rotation [7]	f_{REV}		0	–	4	kHz
Operating Frequency, Nondirection Pulses [7]	f_{ND}		0	–	2.2	kHz
INPUT CHARACTERISTICS AND PERFORMANCE						
Operating Differential Magnetic Input [8]	$B_{DIFF(pk-pk)}$	Differential peak-to-peak magnetic input signal; see Figure 7	5	–	–	G
Operating Differential Magnetic Range [8]	B_{DIFF}	Differential magnetic input range; see Figure 7	–300	–	300	G
Operating Differential Magnetic Offset	$B_{DIFFEXT}$	Differential magnetic offset; see Figure 7	–40	–	40	G
Operating Single-Ended Bx Field Magnitude	B_x	Refer to Figure 8 for field orientations	–50	–	50	G
Operating Magnetic Input Signal Variation	$\Delta B_{DIFF(pk-pk)}$	Bounded amplitude ratio within T_{WINDOW} [9]; no missed output transitions or flat line condition; possible incorrect direction information; see Figure 4 and Figure 5	0.6	–	–	–
Operating Magnetic Input Signal Window	T_{WINDOW}	Rolling window where $\Delta B_{DIFF(pk-pk)}$ cannot exceed bounded ratio; see Figure 4 and Figure 5	3	–	–	T_{CYCLE}
Operate Point	B_{OP}	% of peak-to-peak IC-processed signal	–	70	–	%
Release Point	B_{RP}	% of peak-to-peak IC-processed signal	–	30	–	%
Switch Point Separation	$B_{DIFF(SP-SEP)}$	Required amount of amplitude separated between channels at each B_{OP} and B_{RP} occurrence; see Figure 6	20	–	–	% $B_{DIFF(pk-pk)}$

[7] Maximum Operating Frequency is determined by satisfactory separation of output pulses: $I_{CC(Low)}$ of $t_{w(FWD)(MIN)}$.

[8] Differential magnetic field measured for Channel A (E1-E3) and Channel B (E2-E4) independently; see Figure 11. Magnetic field is measured in the B_y direction; refer to Figure 8 through Figure 10.

[9] Symmetrical signal variation is defined as the largest amplitude ratio from B_n to $B_n + T_{WINDOW}$. Signal variation may occur continuously while B_{DIFF} remains in the operating magnetic range.

Continued on the next page...

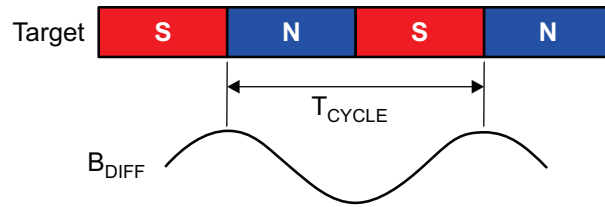
OPERATING CHARACTERISTICS (continued): Valid throughout full operating voltage and ambient temperature ranges, unless otherwise specified

Characteristic	Symbol	Test Conditions	Min.	Typ. [1]	Max.	Unit
THERMAL CHARACTERISTICS						
Magnetic Temperature Coefficient ^[10]	TC	Valid for full temperature range based on ferrite	–	0.2	–	%/°C
Package Thermal Resistance	R _{θJA}	Single-layer PCB with copper limited to solder pads	–	213	–	°C/W
PERFORMANCE CHARACTERISTICS (-xSxxH VARIANTS)						
Vibration Immunity Startup	Err _{VIB(SU)}		2	–	–	T _{CYCLE}
Vibration Immunity Running Mode	Err _{VIB}		2	–	–	T _{CYCLE}
Initial Calibration [11]	T _{CAL}		–	–	4	T _{CYCLE}
First Direction-Pulse Output Following Direction Change [11]			–	–	4	T _{CYCLE}
First Direction-Pulse Output Following Startup Mode Vibration [11]			–	–	4.25	T _{CYCLE}
First Direction-Pulse Output Following Running Mode Vibration [11]			–	–	4.25	T _{CYCLE}
PERFORMANCE CHARACTERISTICS (-xSxxL VARIANTS)						
Vibration Immunity Startup	Err _{VIB(SU)}		0.06	–	–	T _{CYCLE}
Vibration Immunity Running Mode	Err _{VIB}		0.03	–	–	T _{CYCLE}
Initial Calibration [11]	T _{CAL}		–	–	4	T _{CYCLE}
First Direction-Pulse Output Following Direction Change [11][12]			–	–	1.75	T _{CYCLE}
First Direction-Pulse Output Following Startup Mode Vibration [11][12]			–	–	3.75	T _{CYCLE}
First Direction-Pulse Output Following Running Mode Vibration [11][12]			–	–	3.75	T _{CYCLE}

[10] Magnets decrease in strength with increasing temperature. The temperature coefficient compensates to help maintain a consistent maximum air gap over temperature.

[11] Rotational frequencies ≤ 1 kHz. Rotational frequencies above 1 kHz may require more input magnetic cycles until output edges are achieved.

[12] It is possible with the -xxxxL variant to get incorrect direction pulses during direction change and vibration. See Direction Changes, Vibrations, and Anomalous Events section for further details.



T_{CYCLE} = Target Cycle; the amount of rotation that moves one north pole and one south pole across the sensor

B_{DIFF} = Differential Input Signal; the differential magnetic flux density sensed by the sensor

Figure 3: Definition of T_{CYCLE}

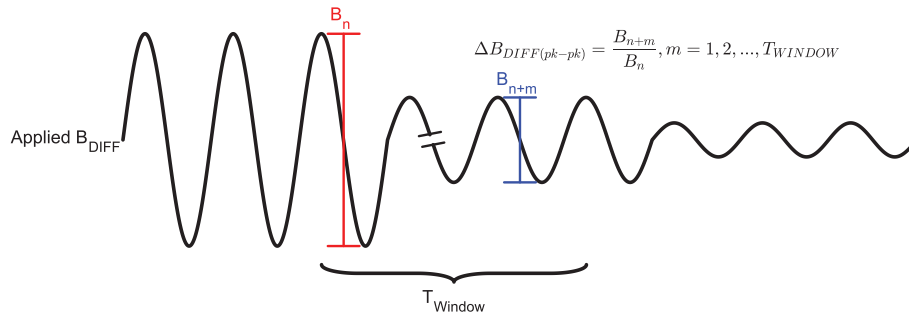


Figure 4: Single Period-to-Period Variation

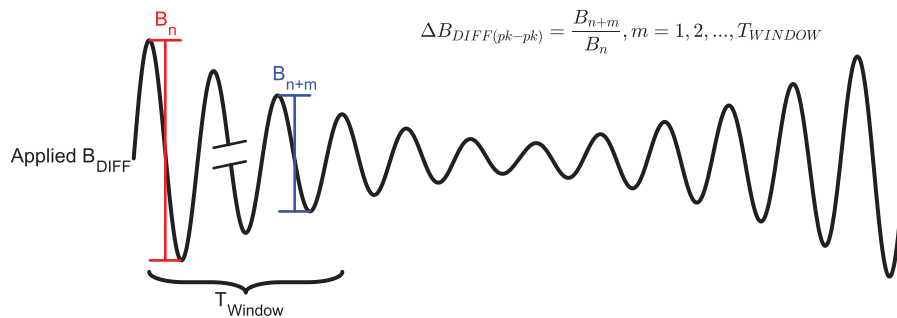


Figure 5: Repeated Period-to-Period Variation

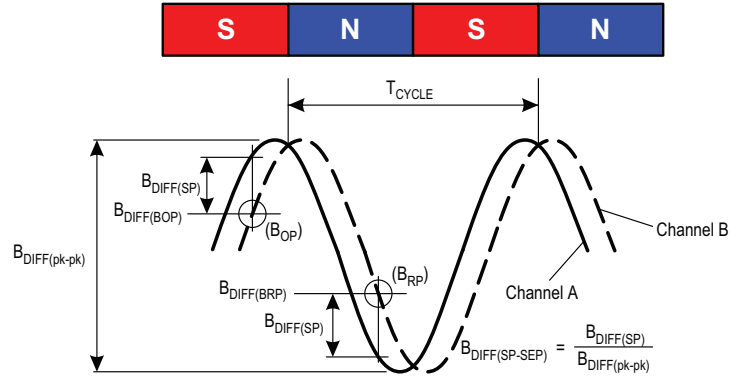


Figure 6: Definition of Switch Point Separation

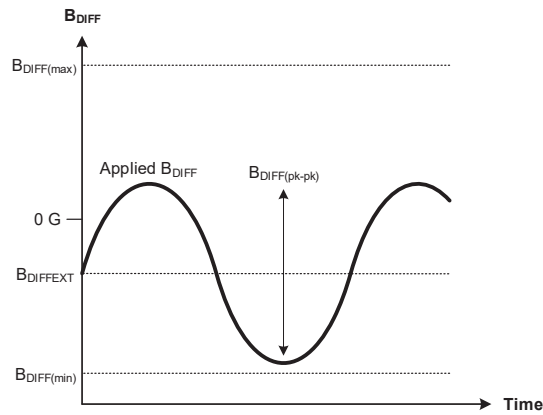


Figure 7: Input Signal Definition

FUNCTIONAL DESCRIPTION

The A19571 sensor IC contains a single-chip GMR circuit that uses spaced elements. These elements are used in differential pairs to provide electrical signals containing information regarding edge position and direction of rotation. The A19571 is intended for use with ring magnet targets.

The IC detects the peaks of the magnetic signals and sets dynamic thresholds based on these detected signals.

Installation Orientation Flexibility

The A19571 can be installed in a parallel, perpendicular, or any orientation in between with respect to the ring magnet. Refer to Figure 8, Figure 9, and Figure 10 for parallel and perpendicular orientations of the sensor.

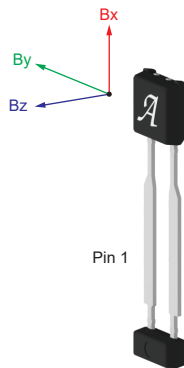


Figure 8: UB Package Orientation

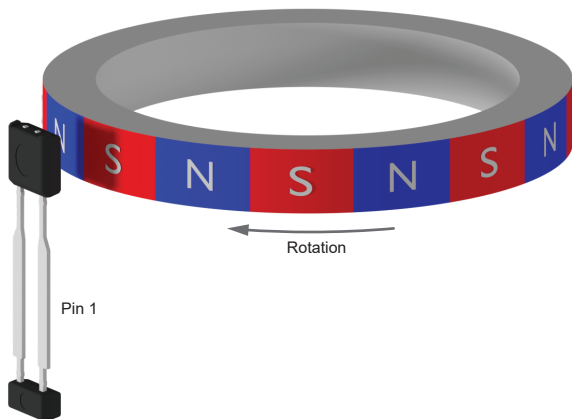


Figure 9: UB Package Parallel Orientation

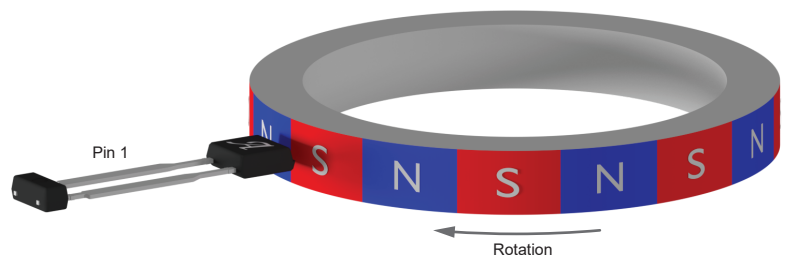


Figure 10: UB Package Perpendicular Orientation

Data Protocol Description

When a target passes in front of the device (opposite the branded face of the package case), the A19571 generates an output pulse for each magnetic pole-pair (-xSxxx variant) of the target. Speed information is provided by the output pulse rate, while direction of target rotation is provided by the duration of the output pulses. The sensor IC can sense target movement in both the forward and reverse directions.

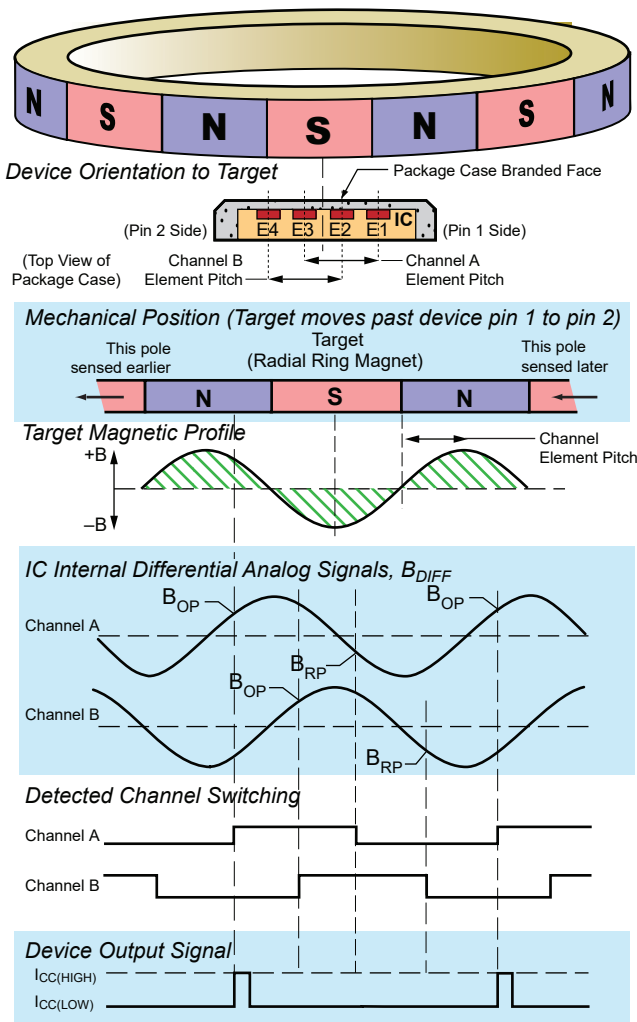


Figure 11: Basic Operation

Forward Rotation. For the -Fxxxx variant, when the target is rotating such that a target feature passes from pin 1 to pin 2, this is referred to as forward rotation. This direction of rotation is indicated on the output by a $t_{W(FWD)}$ pulse width. For the -Rxxxx variant, forward direction is indicated for target rotation from pin 2 to 1.

Reverse Rotation. For the -Fxxxx variant, when the target is rotating such that a target feature passes from pin 2 to pin 1, this is referred to as reverse rotation. This direction of rotation is indicated on the output by a $t_{W(REV)}$ pulse width. For the -Rxxxx variant, reverse direction is indicated for target rotation from pin 1 to 2.

Output edges are triggered by B_{DIFF} transitions through the switch points. On a crossing, the output pulse of $I_{CC(HIGH)}$ is present for $t_{W(FWD)}$ or $t_{W(REV)}$.

The IC is always capable of properly detecting input signals up to the defined operating frequency. At frequencies beyond the operational frequency specifications (refer to Operational Frequency specifications), the $I_{CC(HIGH)}$ pulse duration will collide with subsequent pulses.

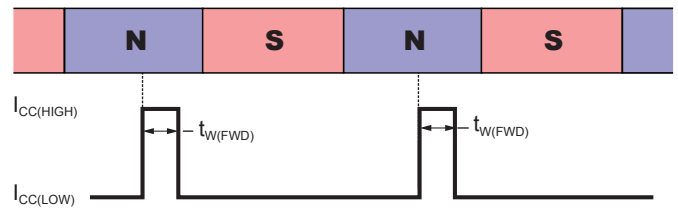


Figure 12: Output Timing Example (-xSxxx variant)

ASIL Safe State Output Protocol

The xxxxx-A variant contains diagnostic circuitry that will continuously monitor occurrences of failure defects within the IC. Refer to Figure 13 for the output protocol of the ASIL safe state after an internal defect has been detected. Warning faults will result from faults due to overfrequency conditions from the input signal. Critical faults will result from hard failures detected within the A19571 such as a regulator and front end fault.

Note: If a fault exists continuously, the device will stay in permanent safe state. Refer to the A19571 Safety Manual for additional details on the ASIL Safe State Output Protocol.

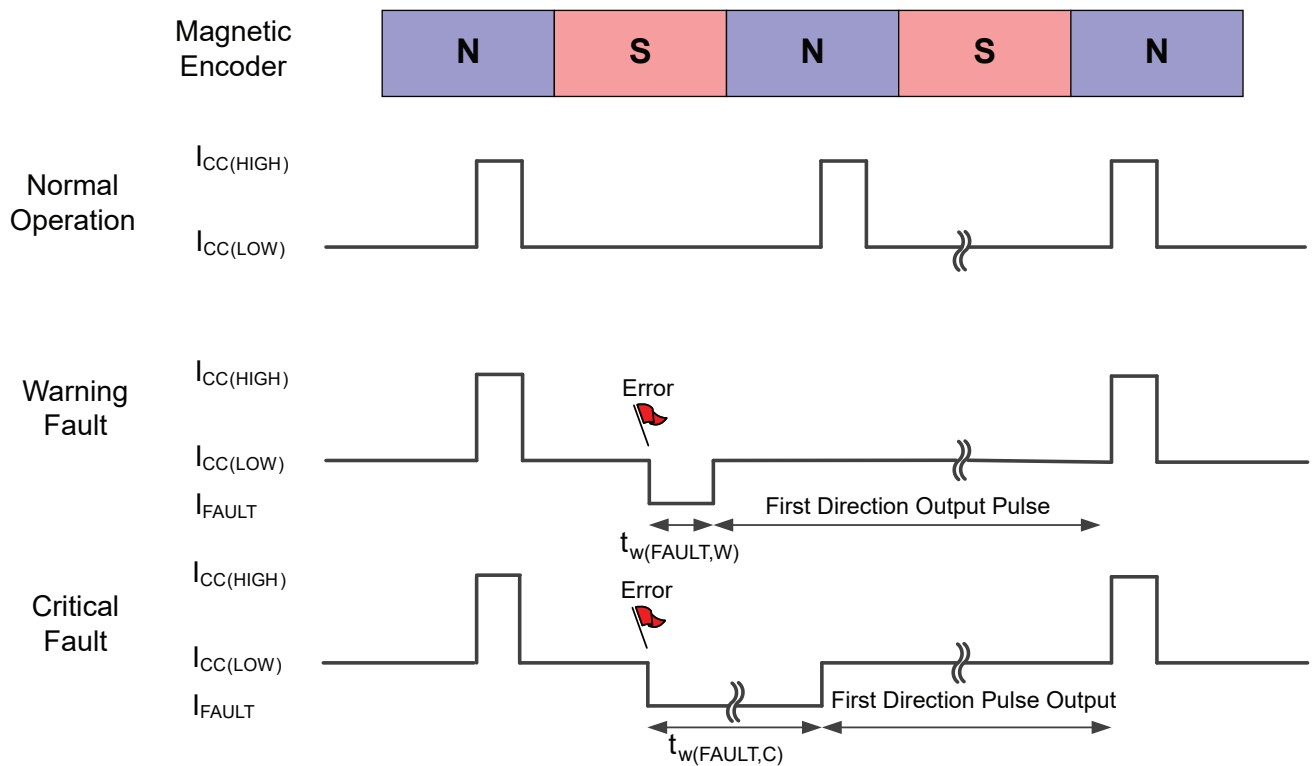


Figure 13: Output Protocol of the -xxxBx-A Variant (ASIL Safe State)

Calibration and Direction Validation

When power is applied to the A19571, the built-in algorithm performs an initialization routine. For a short period after power-on, the device calibrates itself and determines the direction of target rotation. For the -xxxPx variant, the output transmits nondirection pulses during calibration (Figure 14). For the -xxxBx variant, the output does not transmit any pulses during calibration.

Once the calibration routine is complete, the A19571 will transmit accurate speed and direction information.

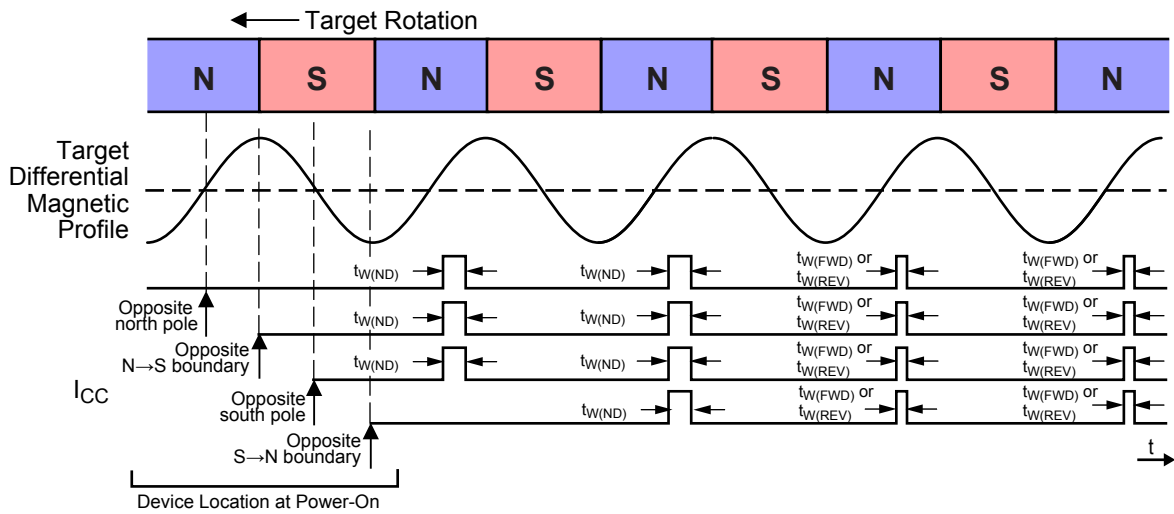


Figure 14: Calibration Behavior of the -xSxPH Variant

Direction Changes, Vibrations, and Anomalous Events

During normal operation, the A19571 will be exposed to changes in the direction of target rotation (Figure 15), vibrations of the target (Figure 16), and anomalous events such as sudden air gap changes. These events cause temporary uncertainty in the A19571’s internal direction detection algorithm.

The -xxxxL variant may output an incorrect direction pulse during direction change and vibration, the -xxxPH variant may transmit nondirection pulses during direction change and vibration, and the -xxxBH variant will not transmit any pulses during direction change and vibration.

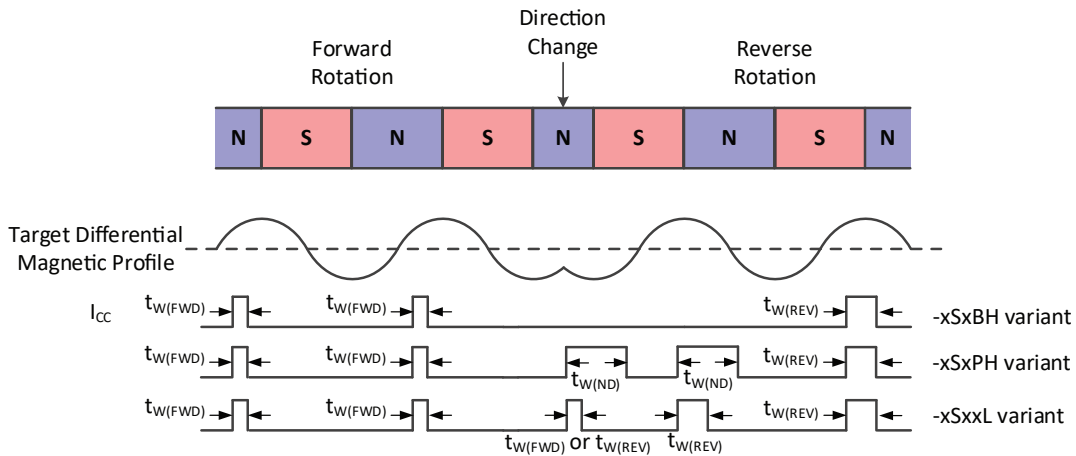


Figure 15: Direction Change Behavior

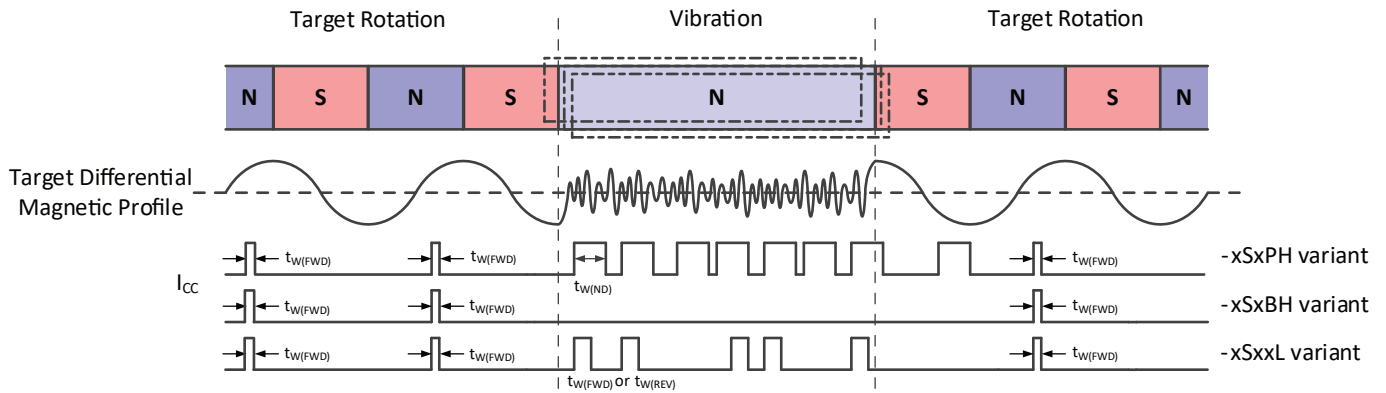


Figure 16: Vibration Behavior

POWER DERATING

The device must be operated below the maximum junction temperature of the device, $T_{J(max)}$. Under certain combinations of peak conditions, reliable operation may require derating supplied power or improving the heat dissipation properties of the application. This section presents a procedure for correlating factors affecting operating T_J . (Thermal data is also available on the Allegro MicroSystems website.)

The Package Thermal Resistance, $R_{\theta JA}$, is a figure of merit summarizing the ability of the application and the device to dissipate heat from the junction (die), through all paths to the ambient air. Its primary component is the Effective Thermal Conductivity, K , of the printed circuit board, including adjacent devices and traces. Radiation from the die through the device case, $R_{\theta JC}$, is a relatively small component of $R_{\theta JA}$. Ambient air temperature, T_A , and air motion are significant external factors, damped by overmolding.

The effect of varying power levels (Power Dissipation, P_D) can be estimated. The following formulas represent the fundamental relationships used to estimate T_J , at P_D .

$$P_D = V_{IN} \times I_{IN} \quad (1)$$

$$\Delta T = P_D \times R_{\theta JA} \quad (2)$$

$$T_J = T_A + \Delta T \quad (3)$$

For example, given common conditions such as:

$T_A = 25^\circ\text{C}$, $V_{CC} = 12\text{ V}$, $R_{\theta JA} = 213^\circ\text{C/W}$, and $I_{CC} = 7.15\text{ mA}$,

then:

$$P_D = V_{CC} \times I_{CC} = 12\text{ V} \times 7.15\text{ mA} = 85.8\text{ mW}$$

$$\Delta T = P_D \times R_{\theta JA} = 85.8\text{ mW} \times 213^\circ\text{C/W} = 18.3^\circ\text{C}$$

$$T_J = T_A + \Delta T = 25^\circ\text{C} + 18.3^\circ\text{C} = 43.3^\circ\text{C}$$

A worst-case estimate, $P_{D(max)}$, represents the maximum allowable power level ($V_{CC(max)}$, $I_{CC(max)}$), without exceeding $T_{J(max)}$, at a selected $R_{\theta JA}$ and T_A .

Example: Reliability for V_{CC} at $T_A = 150^\circ\text{C}$.

Observe the worst-case ratings for the device, specifically:

$R_{\theta JA} = 213^\circ\text{C/W}$ (subject to change), $T_{J(max)} = 165^\circ\text{C}$, $V_{CC(max)} = 24\text{ V}$, and $I_{CC(AVG)} = 15.4\text{ mA}$. $I_{CC(AVG)}$ is computed using $I_{CC(HIGH)(max)}$ and $I_{CC(LOW)(max)}$, with a duty cycle of 92% computed from $t_{w(ND)(max)}$ on-time and $t_{w(FWD)(min)}$ off-time (pulse-width protocol). This condition happens at a select limited frequency.

Calculate the maximum allowable power level, $P_{D(max)}$. First, invert equation 3:

$$\Delta T_{max} = T_{J(max)} - T_A = 165^\circ\text{C} - 150^\circ\text{C} = 15^\circ\text{C}$$

This provides the allowable increase to T_J resulting from internal power dissipation. Then, invert equation 2:

$$P_{D(max)} = \Delta T_{max} \div R_{\theta JA} = 15^\circ\text{C} \div 213^\circ\text{C/W} = 70.4\text{ mW}$$

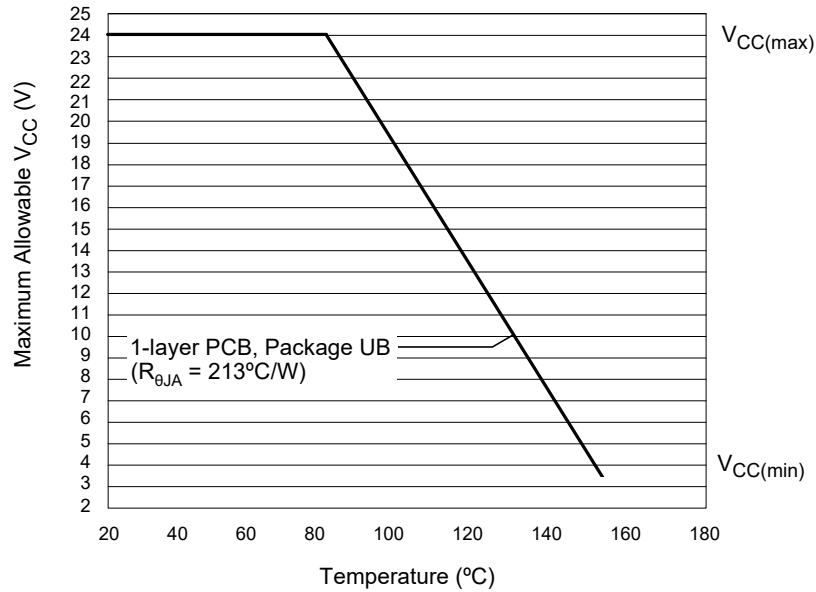
Finally, invert equation 1 with respect to voltage:

$$V_{CC(est)} = P_{D(max)} \div I_{CC(max)} = 70.4\text{ mW} \div 15.4\text{ mA} = 4.6\text{ V}$$

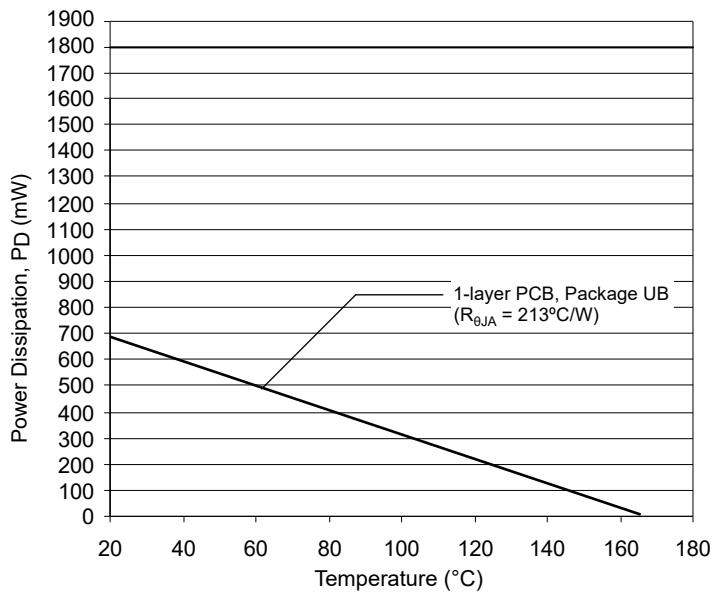
The result indicates that, at T_A , the application and device can dissipate adequate amounts of heat at voltages $\leq V_{CC(est)}$.

Compare $V_{CC(est)}$ to $V_{CC(max)}$. If $V_{CC(est)} \leq V_{CC(max)}$, then reliable operation between $V_{CC(est)}$ and $V_{CC(max)}$ requires enhanced $R_{\theta JA}$. If $V_{CC(est)} \geq V_{CC(max)}$, then operation between $V_{CC(est)}$ and $V_{CC(max)}$ is reliable under these conditions.

Power Derating Curve



Power Dissipation versus Ambient Temperature



PACKAGE OUTLINE DRAWING

For Reference Only – Not for Tooling Use

(Reference DWG-0000408, Rev. 4)

Dimensions in millimeters – NOT TO SCALE

Exact case and lead configuration at supplier discretion within limits shown

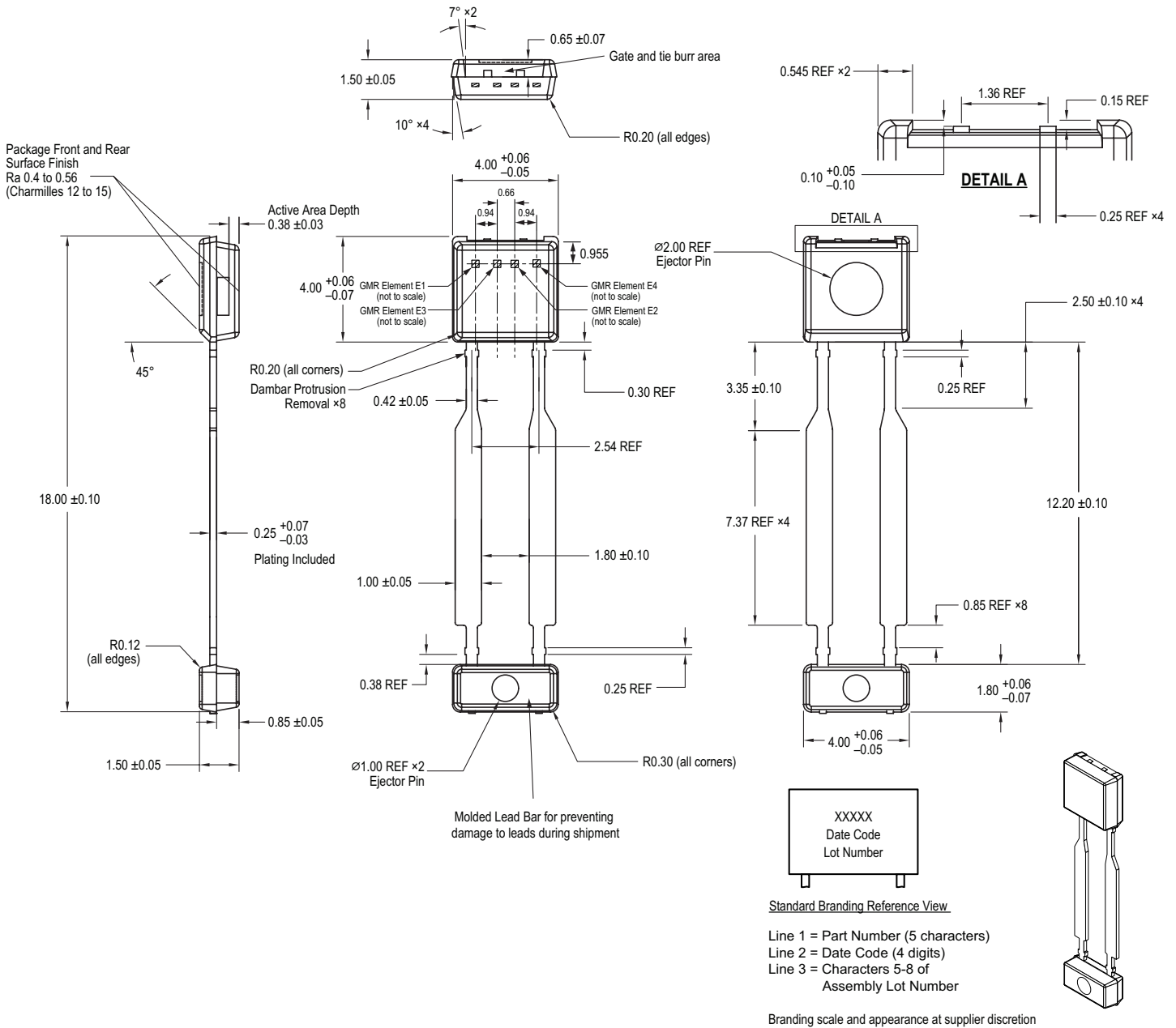


Figure 17: Package UB, 2-Pin SIP

Revision History

Number	Date	Description
–	September 4, 2020	Initial release
1	April 20, 2021	Updated ASIL status (page 1)
2	April 25, 2024	Updated package drawing (page 16)

Copyright 2024, Allegro MicroSystems.

Allegro MicroSystems reserves the right to make, from time to time, such departures from the detail specifications as may be required to permit improvements in the performance, reliability, or manufacturability of its products. Before placing an order, the user is cautioned to verify that the information being relied upon is current.

Allegro's products are not to be used in any devices or systems, including but not limited to life support devices or systems, in which a failure of Allegro's product can reasonably be expected to cause bodily harm.

The information included herein is believed to be accurate and reliable. However, Allegro MicroSystems assumes no responsibility for its use; nor for any infringement of patents or other rights of third parties which may result from its use.

Copies of this document are considered uncontrolled documents.

For the latest version of this document, visit our website:

www.allegromicro.com